Inhibitory Mechanism of Serpins: Loop Insertion Forces Acylation of Plasminogen Activator by Plasminogen Activator Inhibitor-1†

Jan-Olov Kvassman,* Ingrid Verhamme, and Joseph D. Shore

Henry Ford Health Sciences Center, Division of Biochemical Research, Detroit, Michigan

Received June 22, 1998; Revised Manuscript Received August 13, 1998

ABSTRACT: Serpin inhibitors are believed to form an acyl enzyme intermediate with their target proteinases which is stabilized through insertion of the enzyme-linked part of the reactive center loop (RCL) as strand 4 in β-sheet A of the inhibitor. To test critically the role and timing of these steps in the reaction of the plasminogen activator inhibitor PAI-1, we blocked the vacant position 4 in β-sheet A of this serpin with an octapeptide. The peptide-blocked PAI-1 was a substrate for both tissue-type plasminogen activator (tPA) and trypsin and was hydrolyzed at the scissile bond. The reactivity of the peptide-blocked substrate PAI-1 was compared to that of the unmodified inhibitor by rapid acid quenching as well as photometric techniques. With trypsin as target, the limiting rate constants for enzyme acylation were essentially the same with inhibitor and substrate PAI-1 (21−23 s^{-1}), as were also the associated apparent second-order rate constants (2.8−2.9 μM^{-1} s^{-1}). With tPA, inhibitor and substrate PAI-1 reacted identically to form a tightly bound Michaelis complex ($K_d \approx K_m \approx 20$ nM). The limiting rate constant for acylation of tPA, however, was 57 times faster with inhibitor PAI-1 (3.3 s^{-1}) than with the substrate form (0.059 s^{-1}), resulting in a 5-fold difference in the corresponding second-order rate constants (13 vs 2.5 μM^{-1} s^{-1}). We attribute the ability of tPA to discriminate between the two PAI-1 forms to exosite bonds that cannot occur with trypsin. The exosite bonds retain specifically the distal part of the PAI-1 RCL in the substrate pocket, which favors a reversal of the acylation step. Acylation of tPA becomes effective only by separating the products of the acylation step. With substrate PAI-1, this depends on passive displacement of bonds, whereas with inhibitor PAI-1, separation is accomplished by loop insertion that pulls tPA from its docking site on PAI-1, resulting in faster acylation than with substrate PAI-1.

The serine proteinase inhibitors of the serpin family are a homogenous group of proteins which regulate the proteolytic cascades in processes such as coagulation, fibrinolysis complement activation, and inflammation (*1*). The most conspicuous structural elements of the serpin are an extended and flexible reactive center loop (RCL) and a large β-sheet (sheet A) (*2*), both intimately linked to the function of the inhibitor (*3*, *4*). The RCL is a direct continuation of β-strand 5A and is also firmly anchored to the protein scaffold at its C-terminal side. It contains about 20 residues (P15−P4′) and exposes the reactive center (P1−P1′) at the apex of the slightly elongated molecule. The serpin gains substantial thermodynamic stability by inserting the N-terminal P15−P3 part of the RCL into the normally vacant position 4 of sheet A, making this sheet 6-stranded and overall antiparallel (*5*, *6*). In the intact inhibitor, loop insertion is prevented or hindered by a high kinetic barrier, but upon hydrolysis of the RCL at or near the reactive center, loop insertion is swift and irreversible. There are strong indications that the mechanism of serpin action involves cleavage of the P1−P1′ reactive center bond through acylation of the enzyme active site serine residue (*7*, *8*) and is associated with either complete or partial insertion of the N-terminal (proximal) part of the RCL (carrying the proteinase at its C-terminus) as strand 4 in sheet A (*9*−*11*). This would make the serpin a suicide substrate inhibitor (*12*) which adds a dead end branch to an otherwise normal cycle of serine proteinase peptide hydrolysis (*13*). This concept of the serpin mechanism is illustrated by the mechanism in Scheme 1 (*14*, *15*). In this scheme, I is the serpin; E, the proteinase; EI, the noncovalent (Michaelis) complex, E∼I, the acyl enzyme intermediate, E−I, the stabilized form of the acyl enzyme; and I*, the scissile bond hydrolyzed serpin. Serpin inhibitory efficiency (except for a possible breakdown of the stabilized complex) depends on the relative magnitudes of k_3 and k_4, considered to be controlled by hydrolysis of the acyl enzyme intermediate and loop insertion in the inhibitor, respectively.

Scheme 1

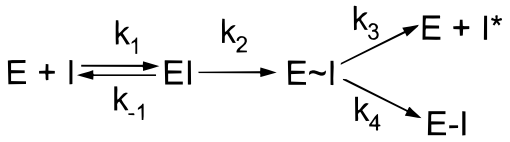

Despite a broad consensus on the mechanism in Scheme 1, uncertainties persist about what triggers insertion of the RCL into sheet A, whether it occurs in a single step, what type of complex it leads to, and how this step can so efficiently arrest the catalytic reaction in competition with

† This work was supported by grant HL45930A07 (J.D.S.) from the National Institutes of Health and grant-in-aid 30GS9789 (J.-O.K.) from the American Heart Association of Michigan.

* Address: One Ford Place, 5D, Detroit, MI 48202-3450. Tel: 313-876-3196 (7291). Fax: 313-876-2380. E-mail: jkvassm1@hfhs.org.

10.1021/bi9814787 CCC: $15.00
Published on Web 10/17/1998

the usually fast deacylation by bulk water. Apart from a study involving the RCL P9 Ser→Cys mutant form of the plasminogen activator inhibitor PAI-1, carrying a fluorescent label at the mercapto group (*9*), no experiment has been described that elucidates the kinetics of loop insertion in the serpin reaction. There are several reasons why further studies of PAI-1 could provide valuable mechanistic information. This serpin is a fast and efficient inhibitor of its primary physiological targets, the tissue- and urinary-type plasminogen activators (tPA and uPA), as well as of trypsin. Of particular importance for the present study is the fact that tPA and PAI-1 have developed exosite interactions which enhance formation of the tPA·PAI-1 Michaelis complex and reduce its K_d to the nanomolar range (*16*). On the tPA side, the exosite interactions appear to be mediated predominantly by a series of positively charged side chains which are located in a surface loop (the "37-loop") such that they could promote docking of PAI-1 to tPA by interacting with complementary side chains in or near the distal part of the PAI-1 RCL (*17*, *18*). Consistent with this idea is the fact that when the corresponding sequence in the 37-loop of thrombin was replaced by that of tPA, it resulted in a 2000-fold increase in the second-order rate constant for PAI-1 binding to thrombin (*19*).

Specific evidence that Arg-39 of tPA forms a salt bridge to the glutamate at P4′ in the PAI-1 RCL has been presented (*20*, *21*). This salt bridge was modeled on the basis of an analogous interaction in the complex of trypsin with the canonical pancreatic trypsin inhibitor (*17*), which is noncovalent in nature and is characterized by an intact reactive center bond. By analogy, acylation of tPA by PAI-1 could be reversed through a fast deacylation by the retained P1′ α-amino group and become effective only when the distal part of the cleaved RCL is separated from the tPA substrate pocket. Hence, loop insertion and the concomitant translocation of the proteinase to its ultimate "locking site" may determine the acylation rate and the overall reactivity of PAI-1 with tPA. According to the irreversible acylation mechanism in Scheme 1, however, loop insertion can have no effect on the rate by which the serpin acylates its target.

For the purpose of studying the effects of loop insertion on serpin reactivity, PAI-1 has the additional advantage that a loop-mimicking peptide can be bound easily to the vacant crevice for strand 4 in its β-sheet A, resulting in a species of high thermodynamic stability that is also a substrate for the target proteinases and hydrolyzed at the scissile bond (*4*). Limited hydrolysis of the active serpin in its reaction with the target proteinase is considered to result from lack of loop insertion. The corresponding reaction of the PAI-1 substrate form, in which loop insertion is prevented, should therefore be a suitable model for the proteolytic branch of the bifurcation scheme and could provide information about the role and timing of loop insertion in the PAI-1 reaction. In particular, if acylation of tPA by PAI-1 depends on separating a tightly bound distal peptide fragment from the proteinase substrate pocket, as suggested above, acylation of tPA should be slower with the substrate form than with inhibitor PAI-1 due to the fact that, with substrate PAI-1, the highly exergonic and potentially rapid step of loop insertion cannot facilitate this separation.

In this study, we have used PAI-1 and a substrate form of the inhibitor, created by blocking position 4 of its β-sheet A with the octapeptide Ac-TVASSSTA (cf. P14−P7 of the PAI-1 RCL), to test critically the role and timing of loop insertion in the reactions of PAI-1 with tPA and trypsin. Trypsin was included as reference target because, besides being a well-studied serine proteinase, it lacks the residues implicated in the tPA exosites for PAI-1 (*20*) and yet is rapidly inhibited by this serpin. The rapid acid quenching technique (*22*), which we have used in a previous study on PAI-1 (*23*), was applied to obtain direct information on the rates of enzyme acylation and the overall reactivity with the two PAI-1 forms. Photometric techniques were applied to obtain complementary kinetic information. Our results show that acylation of tPA by PAI-1 is much slower when loop insertion is blocked, consistent with a reversible acylation of the enzyme. They also show that acylation of tPA is unfavorable (Scheme 2), and indicate that this is due to exosite interactions involving the distal part of the PAI-1 RCL. The opposite observation that trypsin was acylated

Scheme 2

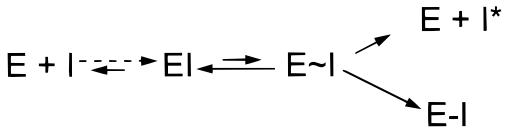

at the same rate by the two PAI-1 forms emphasizes that the exosite bonds have evolved to boost the reactivity toward PAI-1 of a relatively inert and highly selective tPA and that the residues responsible are absent or different in trypsin. In contrast to data showing that the RCL of the serpin antithrombin III is partly inserted into position 4 of its β-sheet A (*24*−*26*), data presented here indicate that the PAI-1 RCL is fully extracted from β-sheet A in the free inhibitor as well as in the Michaelis complexes with tPA and trypsin.

MATERIALS AND METHODS

The chromogenic substrates S2222,[1] S2251, and S2288 were obtained from Chromogenix (Mölndal, Sweden) and were dissolved in 1 mM HCl to a concentration of 5 mM. Spectrozyme^{tPA} was obtained from American Diagnostica and dissolved in water to a concentration of 10 mM. Hydrolysis of the chromogenic substrates was monitored spectrophotometrically at 405 nm and quantitated using an extinction coefficient of 10^4 M^{-1} cm^{-1} for *p*-nitroaniline. If not otherwise indicated, measurements were performed at pH 7.5 and 25 °C in a standard buffer prepared with analytical grade HEPES (30 mM) and NaOH (15 mM) dissolved in deionized, distilled, and degassed water and adjusted to 0.15 M ionic strength with NaCl.

Proteins. Human recombinant PAI-1, expressed in *E.coli*, and bovine β-trypsin were obtained, purified, and analyzed as previously described (*4*). Human recombinant tPA

[1] Abbreviations: S2222, *N*-benzoyl-L-isoleucyl-L-glutamyl-glycyl-L-arginine-*p*-nitroanilide; S2251, *H*-D-valyl-L-leucyl-L-lysine-*p*-nitroanilide; S2288, *H*-D-isoleucyl-L-prolyl-L-arginine-*p*-nitroanilide; Spectrozyme^{tPA}, methyl-sulfonyl-D-cyclohexyltyrosyl-glycyl-L-arginine-*p*-nitroanilide; HEPES, 4-(2-hydroxyethyl)piperazine-1-ethanesulfonic acid; MES, 2-morpholinoethanesulfonic acid; BICINE, *N*,*N*-bis(2-hydroxyethyl)glycine; bis-TRIS, bis(2-hydroxyethylamino)-tris(hydroxymethyl)methane; CAPS, 3-(cyclohexylamino)-1-propanesulfonic acid; CHES, 2-(cyclohexylamino)ethanesulfonic acid; MOPS, 3-morpholinopropanesulfonic acid.

(Activase) was kindly provided by Dr. Bruce Keyt at Genentech Inc., San Francisco, CA, USA. The predominantly single-chain tPA (10 mg) was converted to the two-chain form (tc-tPA) by treatment with immobilized plasmin (*27*). The treatment was interrupted when the amidolytic activity of tPA, measured with S2288 (0.1 mM), began to decline slowly after reaching a peak of about 5 times its initial value. Analysis by reducing SDS−PAGE indicated that conversion of sc-tPA to the two-chain form was complete at this stage and that unspecific degradation of tPA was insignificant. The activated enzyme was precipitated by dialysis against solid ammonium sulfate to a final salt saturation of 90%. The precipitate was collected by centrifugation, dissolved in 1.5 mL of 0.15 M NaCl, and desalted on a PD-10 column (Pharmacia) equilibrated with the same solution to which 0.02 M ϵ-aminocaproic acid was added to reduce aggregation of tPA. The tc-tPA thus prepared and then frozen was aggregated when thawed, and before use, the enzyme was redissolved by incubation at 37 °C for 5 min. The concentration of tPA was determined spectrophotometrically at 280 nm using an extinction coefficient of 1.9 mg^{-1} mL cm^{-1} and a M_r of 63 500. All protein solutions were stored frozen at −70 °C.

Peptide-Blocked Substrate PAI-1. The complex of PAI-1 and Ac-TVASSSTA, which functions as a substrate for tPA (*4*), was prepared by mixing 0.5 mL of 80 μM PAI-1, contained in 0.35 M NaCl, 1 mM EDTA, and 5 mM NaH_2PO_4 (pH 6.2), with 0.5 mL of a solution containing 2 mM peptide in the standard HEPES buffer. The mixture was incubated for 20 h at room temperature and subsequently desalted on a PD-10 column (Pharmacia) equilibrated with a solution containing 0.5 mM MES, 0.25 mM NaOH, and 0.15 M NaCl (pH 6.2). The concentration of peptide-blocked PAI-1 was determined spectrophotometrically using the extinction coefficient reported for active PAI-1 (*28*) and corrected for the presence of inactive PAI-1 (∼5%) which was not hydrolyzed by tPA and which was quantitated by SDS−PAGE. We have previously shown that binding to PAI-1 of octapeptides analogous to P14−P7 of the PAI-1 RCL occurs in direct competition with spontaneous loop insertion, forming latent PAI-1, and we concluded that these peptides bind as β-strand 4A (*4*). In the same study, we demonstrated that dialysis of the peptide-complexed PAI-1 for several days with frequent changes of the external solution did not appreciably decrease the proportion of substrate PAI-1, showing that dissociation of the complex is much slower than the spontaneous folding of PAI-1 to form the latent inhibitor.

Rapid Quenching Technique. Rates of proteinase acylation by PAI-1 and peptide-complexed substrate PAI-1 were measured with the rapid acid quenching technique (*22*). The quenching apparatus was built on site and could be operated in continuous-flow mode or pulsed-flow mode with intermittent incubation of reactants (Supporting Information available). The acidic samples collected in the rapid quenching experiments, containing 1% SDS, were briefly heated to boiling, mixed with concentrated electrophoresis treatment buffer, neutralized with 0.5 M NaOH, and subsequently applied to a polyacrylamide gel (9% or 12%) for separation of the reaction components under nonreducing conditions. Typically, 30 μL of the quenched and denatured reaction mixtures, containing 0.5−1.0 μg of the limiting reactant, was applied to each 1.5 mm × 3 mm well of the stacking gel, resulting in bands stained to a peak absorbance less than 1.2.

Protein Quantitation by SDS−PAGE. The electrophoresis gels were stained overnight with Coomassie Brilliant Blue R. After being thoroughly destained, they were placed on top of a light box, and excessive portions of the box were masked with a black cloth. Digital images of the transilluminated gels were recorded in the dark using a CCD camera equipped with a close-up lens. Image data was analyzed using commercial scanning software (Sigmascan, Jandel Scientific, San Rafael, CA). The transmission reported by each pixel of the image was converted to absorbance units using $A = -\log((\text{8-bit pixel intensity})/255)$. A band of protein (comprising 500−2500 pixels) was analyzed by creating a rectangular area that extended into the background above and below the band and covered the lateral edges of the band completely. The average absorbance reported by each horizontal row of pixels across the rectangle was recorded from top to bottom and transferred to a linear plot. A cubic polynomial was fitted to portions of the plot judged to constitute background absorbance, and using the best-fit coefficients, a background absorbance was interpolated over the entire scan and subtracted from the data. The corrected peak was integrated, and the total absorbance was multiplied by the width (in pixels) of the scanned rectangle to correct for differences in bandwidth. The value obtained was taken to be proportional to the mass of the specific protein contained in the analyzed band. This assumption was corroborated by reacting PAI-1 (2 μM) with trypsin (1 μM) and tPA (1 μM) and analyzing increasing amounts of the mixtures by SDS−PAGE. Plots of relative protein mass, determined as described above, against the volume applied was linear for all species tested (i.e., the stable complexes and the intact and cleaved inhibitor) covering the absorbance range 0.1−1.4.

Data Evaluation. Unless otherwise indicated, the data collected for the reactions of inhibitory and substrate PAI-1 with tPA and trypsin were analyzed primarily in view of a two-step mechanism, analogous to the Michaelis−Menten scheme for enzyme action. Two kinetic parameters for each reaction system were determined: (I) the apparent second-order rate constant for the overall reaction which we denote k_{app} and (II) the associated limiting rate constant which we denote k_{lim}. Note that with the substrate form of PAI-1, k_{lim} equals k_{cat} and k_{app} equals k_{cat}/K_m. When required, k_{inh} and k_{cat} will be used to distinguish k_{lim} for inhibitor and substrate PAI-1, respectively. If not otherwise indicated, reaction progress curves were analyzed by nonlinear least-squares fitting of the parameters of a first-order reaction.

Limiting Rate Constants for Enzyme Acylation by Inhibitor and Substrate PAI-1. The trypsin reaction with active PAI-1 was studied by the rapid acid quenching technique in the continuous-flow mode. Trypsin, 10 or 20 μM in 0.15 M NaCl and 1 mM HCl (to preserve the integrity of the enzyme), was reacted with 1 μM PAI-1 in 60 mM HEPES, 30 mM NaOH, and 0.12 M NaCl (pH = 7.5). The reaction was quenched with HCl sufficient to bring the quenched solution to a pH of 2 ± 0.1. The progress of the reaction at the time of quenching was determined by SDS−PAGE as described above. To exclude the possibility that the reactivity of trypsin was limited by conformational changes, caused by jumping the enzyme from pH 3 to pH 7.5 in mixer 1, a

solution with 0.2 μM trypsin in 0.15 M NaCl and 1 mM HCl was mixed in a Durrum stopped-flow spectrophotometer with an equal volume of 0.2 mM S2222 contained in 60 mM HEPES, 30 mM NaOH, and 0.12 mM HCl, and the resulting transmission change at 405 nm was recorded. This control showed that the catalytic activity of trypsin, when jumped from pH 3 to pH 7.5, is not limited by a step slower than 100 s^{-1}.

Formation of the stable tPA•PAI-1 complex was likewise monitored by using the continuous-flow rapid acid quenching technique combined with SDS−PAGE. With both tPA and PAI-1 contained in 30 mM HEPES, 15 mM NaOH, and 135 mM NaCl, the plasmin-activated tPA (2 μM) was reacted with PAI-1 (4 μM) and the reaction was quenched with the solution described above for the reaction with trypsin.

Rates of acylation of tPA and trypsin by the peptide blocked substrate form of PAI-1 were measured with the rapid quenching technique, applied in the pulsed-flow mode when tPA was the target and in the continuous-flow mode when the faster reaction with trypsin was studied. In both cases, the conditions were chosen to monitor a single enzyme turnover and to attempt to saturate the reaction. This was done by reacting 3 μM tPA with 2 μM substrate PAI-1 and 5−20 μM trypsin with 1.6−3.0 μM substrate PAI-1.

Apparent Second-Order Rate Constants for Binding of Inhibitor and Substrate PAI-1 to Trypsin and tPA. The apparent bimolecular rate constants, k_{app}, for the irreversible binding of inhibitor PAI-1 to trypsin and tPA were determined by using the competitive kinetic method with chromogenic substrate (*29*). Trypsin (8 nM) was reacted with PAI-1 (40−80 nM) in the presence of 0.1 mM S2222. The resulting absorbance progress curves were analyzed as single exponentials, and values for k_{app} were evaluated on the basis of the observed rate constants and the inhibitor concentration used and by correcting for the competitive effect of the chromogenic substrate. For the reaction of PAI-1 with tPA, the corresponding rate constant was determined by reacting PAI-1 (20−50 nM) with tc-tPA (4 nM) in cuvettes coated with poly(ethylene glycol) 20 000 to prevent adsorption and by using Spectrozyme^{tPA} (0.5 mM) as reporter substrate.

The k_{app} for the binding of substrate PAI-1 to trypsin was evaluated as k_{cat}/K_m on the basis of direct measurement of V_{max}/K_m. For this purpose, substrate PAI-1 (1 μM) was reacted with catalytic amounts of trypsin (0.065 μM). The reaction was quenched with acid at intervals over a period of 15 s, and the progress of the reaction was determined by SDS−PAGE. Due to much lower values of k_{cat} and K_m for the hydrolysis of substrate PAI-1 by tPA than by trypsin, this reaction was monitored indirectly by using the competitive hydrolysis of Spectrozyme^{tPA} as a reporter reaction (*30*, *31*) and V_{max} and K_m were determined individually. The enzyme (0.005 μM) was mixed with Spectrozyme^{tPA} (15 μM) in the absence and presence of PAI-1 complexed with Ac-TVASSSTA (0.1 and 0.2 μM), and the complete hydrolysis of the chromogenic substrate was monitored spectrophotometrically. Steady-state kinetic parameters for the hydrolysis of substrate PAI-1 were determined by fitting the implicit function in eq 1 (*32*) to the resulting absorbance progress curves. In eq 1, A_i is the registered absorbance, A_∞, its final value, V_s and K_s are V_{max} and K_m for the chromogenic substrate, V_b and K_b are the corresponding parameters for substrate PAI-1, and B_0 is the initial concentration of substrate PAI-1.

$$A_i = A_\infty - V_s t + K_s \ln\frac{A_\infty}{A_i} + \frac{B_0}{V_b}\left(\frac{A_i}{A_\infty}\right)^{(K_s V_b)/(V_s K_b)} \quad (1)$$

Comparison of the Effects of pH on the Amidolytic Activity of tPA and Trypsin. The k_{cat}/K_m for the hydrolysis of S2222 by tPA and trypsin were determined in the pH range 4−11. Measurements were performed in buffered solutions adjusted to an ionic strength of 0.15 M with NaCl. The following substances were used to control pH: acetic acid (pH 4.5−5.5), succinic acid (pH 4.8−5.8), MES (pH 5.6−6.6), bis-TRIS (pH 6−7), MOPS (pH 6.5−7.5), HEPES (pH 7−8), BICINE (pH 8−9) CHES (pH 8.5−9.5), and CAPS (pH 10−11). Data were obtained by reacting 0.07 μM tPA or 0.008 μM trypsin with subsaturating concentrations of S2222 (i.e., 40 μM with tPA and 4 μM with trypsin). The rate constants ($k_{obs} = V_{max}/K_m$) of the resulting exponential progress curves were evaluated by nonlinear regression, and the corresponding apparent second-order rate constants (k_{cat}/K_m) were obtained by dividing k_{obs} by the respective enzyme concentration.

RESULTS

Evaluation of the Rapid Acid Quenching Technique. In the serine proteinase-catalyzed reactions, both acylation and deacylation of the enzyme active site serine residue depend on base catalysis[2] by a neutral His-57.[3] Kinetic as well as structural data on trypsin and chymotrypsin indicate that His-57 is accessible for protonation in all major intermediates of the catalytic reaction and exhibits pK_a values in the neutral pH range (*33*−*36*). Acidification of the reaction medium should therefore exert an immediate effect on the catalytic machinery of both the free and bound serine proteinase by protonating His-57 and deactivating it as a base catalyst. If the pK_a of His-57 is not lower than 6, the rates of acylation and deacylation should be reduced by a factor 10^4 or more when the system is quenched with acid to a final pH of 2. This should provide sufficient prevention of enzyme acylation and deacylation until secondary effects of the low pH[4] or the addition of SDS dissociate the noncovalent complexes and denature both enzyme and inhibitor. Several control experiments were performed to evaluate this assumption. In one control, the addition of SDS was omitted until the samples had been incubated at pH 2 for periods ranging from 10 to 30 min. The time courses observed for enzyme acylation were not significantly different from those observed when SDS was included in the collecting tubes and hence added to the quenched mixtures after only a few milliseconds. In a second control, SDS (1%) was used as the single agent to quench the reaction at pH 7.5. Although this led to the appearance in the gels of more of the hydrolyzed inhibitor

[2] This apparent contradiction of the Onsager principle of microscopic reversibility has been resolved by the introduction of tetrahedral intermediates, the breakdown of which—to the acyl enzyme intermediate or the free enzyme and substrate or product—depends on acid catalysis by the protonated form of His-57.

[3] Serine proteinase residues are identified according to their position in chymotrypsinogen.

[4] The dissociating effect of low pH is demonstrated by the fact that the trypsin used in this study was eluted from a column with immobilized soybean trypsin inhibitor by a pH gradient ranging from 4.7 to 2.

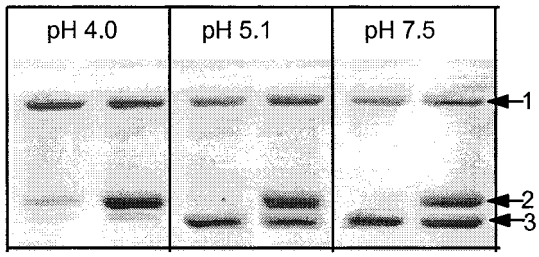

FIGURE 1: Apparent variation with pH of the proportion inhibitor PAI-1 that is hydrolyzed by trypsin. The left lane in each pH section of the gel was obtained using 2 μM trypsin and 1 μM PAI-1, whereas the right lanes were obtained using 1 μM trypsin and 2 μM PAI-1. When the reactions were complete (almost complete at pH 4 and 5.1), the proteins were denatured by addition of 1% SDS followed by heating to 100 °C. The samples were adjusted to pH 7.5, and treatment buffer containing glycerol and tracking dye was added to the samples before they were applied to the gel. The bands are (1) the trypsin·PAI-1 complex, (2) unreacted PAI-1, and (3) PAI-1 hydrolyzed at the scissile bond.

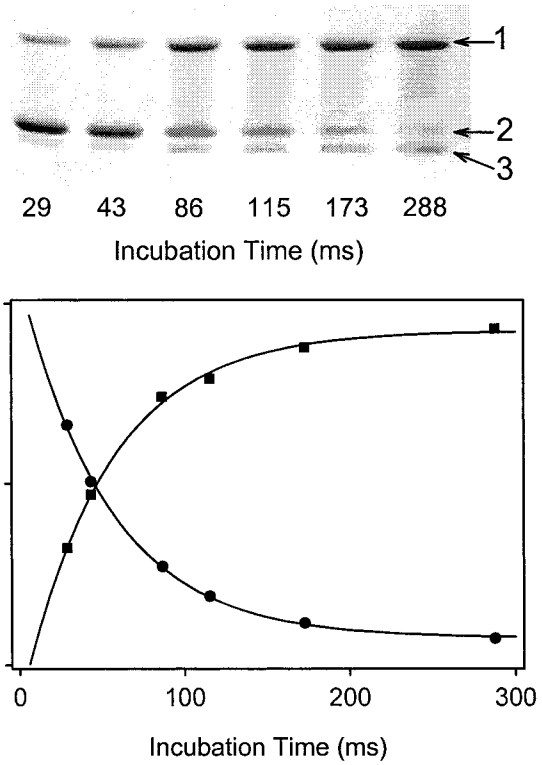

FIGURE 2: Formation of the stable trypsin·PAI-1 acyl enzyme intermediate under close to saturating conditions. Trypsin (10 μM) was reacted with inhibitor PAI-1 (1 μM), and the reaction was quenched at pH 2 after the indicated times of incubation. The components of the quenched reaction mixtures were separated by SDS−PAGE into (1) the trypsin·PAI-1 complex, (2) unreacted and noncovalently bound PAI-1, and (3) PAI-1 hydrolyzed at the scissile bond (trypsin migrated with the dye front). The bands were individually quantitated, and the trypsin·PAI-1 complex (■) as well as unreacted PAI-1 (free and noncovalently bound) (●) were plotted against time. The solid lines correspond to the best fit exponential rate constants $k_{obs} = 18.9 \pm 1.5$ s^{-1} (trypsin·PAI-1) and $k_{obs} = 18.9 \pm 0.9$ s^{-1} (unreacted PAI-1).

and less of the stabilized complex, specifically when trypsin was the target (see comments below), the time courses of enzyme acylation were the same. To ascertain that tPA does not deviate from trypsin with regard to the role and pK_a of His-57, the pH profiles of k_{cat}/K_m for hydrolysis of the chromogenic substrate S2222 by plasmin-activated two-chain

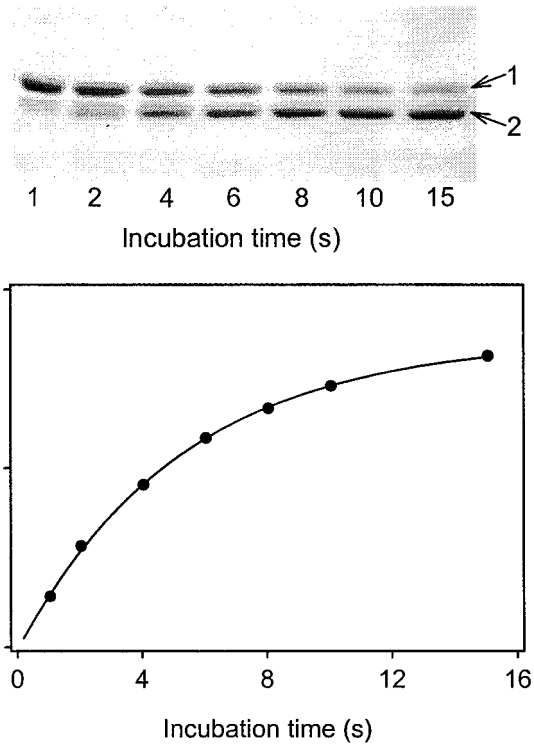

FIGURE 3: First-order hydrolysis of substrate PAI-1 by catalytic amounts of trypsin. PAI-1 complexed with Ac-TVASSSTA (1 μM) was reacted with trypsin (0.065 μM), and the reaction was quenched at pH 2 after the indicated times of incubation. Intact (1) and scissile bond hydrolyzed PAI-1 (2) were separated by SDS−PAGE, and the bands were quantitated as described in the Experimental Section. The relative amounts of hydrolyzed PAI-1 were plotted against time. The solid line represents a single exponential with the rate constant $k_{obs} = 0.19 \pm 0.01$ s^{-1}.

tPA and trypsin were determined. When normalized, the bell-shaped profiles were nearly identical, indicating that ionization of His-57 (and the Ile-16 α-amino group) has the same effect on the overall activity of two-chain tPA as it has on trypsin and occurs with virtually the same pK_a value (6.9 versus 6.8).

When quenched by acid and analyzed by SDS−PAGE, the reaction between inhibitor PAI-1 and proteinase appeared to result in minor amounts of PAI-1, hydrolyzed at the scissile bond (Figures 2 and 5), consistent with the bifurcation scheme for serpin action. However, the proportion of hydrolyzed inhibitor observed varied depending on how the samples had been prepared for SDS−PAGE. Data presented in Figure 1 gives the impression that half or more of the PAI-1 is hydrolyzed when reacted with trypsin at pH 7.5. Most of the hydrolyzed inhibitor, however, resulted from hydrolysis of the stabilized complex induced by SDS at pH 7.5, as demonstrated by the much smaller proportion generated when the reaction was run at pH 7.5 but denatured with SDS at pH 2 (Figure 2) and by titration of trypsin activity with PAI-1, which indicated a stoichiometry of inhibition indistinguishable from 1:1. However, no evidence was obtained that hydrolysis of the stable complex was completely abolished by adding SDS at pH 2. Consequently, we will refrain from using the proportion of hydrolyzed PAI-1 as a measure of PAI-1 inhibitory efficiency. The exceptions are justified by the fact that the amount of hydrolyzed PAI-1 observed in the gels is always equal to or larger than that generated by the substrate branch of the

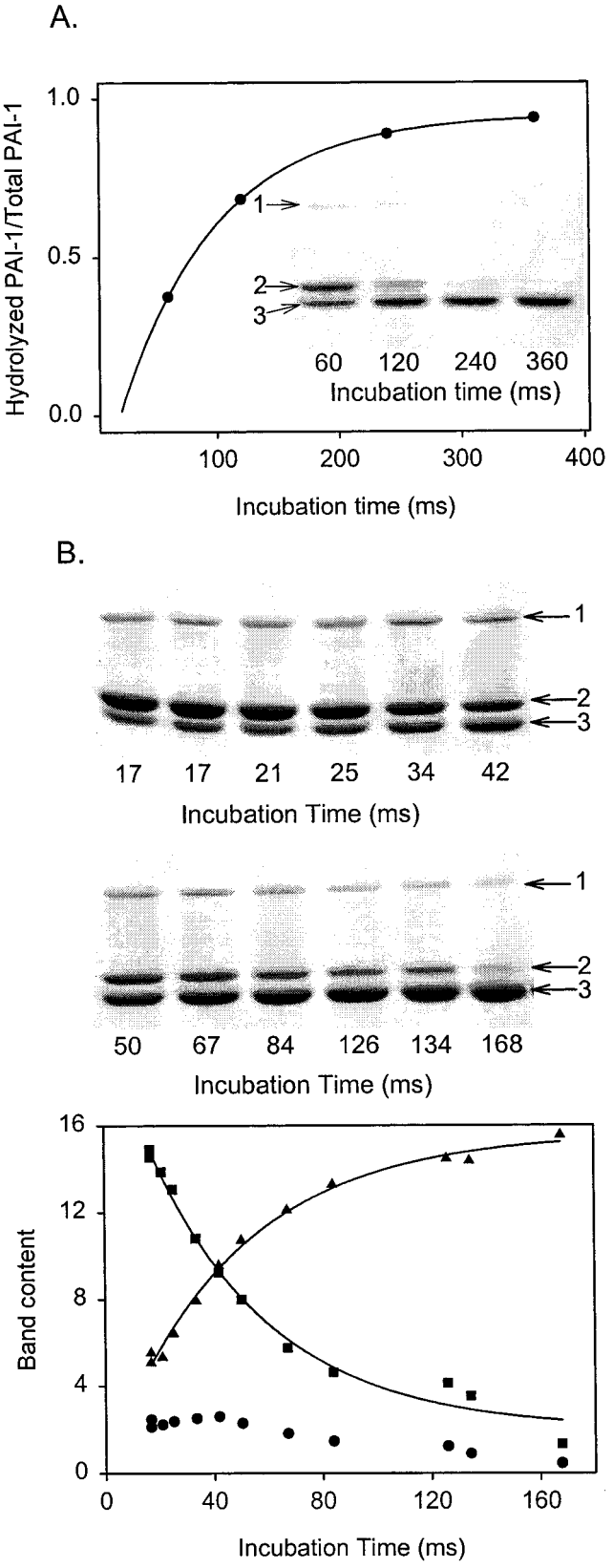

FIGURE 4: Time course for hydrolysis of substrate PAI-1 by trypsin under single turnover conditions. (a) Trypsin (5 μM) was reacted with Ac-TVASSSTA-complexed PAI-1 (1.6 μM), and the reaction was quenched at pH 2 after the indicated times of incubation. The reaction components were separated by SDS−PAGE into (1) the acyl enzyme intermediate, (2) intact unreacted and noncovalently bound PAI-1, and (3) PAI-1 hydrolyzed at the scissile bond. The relative amounts of the latter were plotted against time. The solid line represents a single exponential with the rate constant k_{obs} = 12.7 ± 0.3 s^{-1}. (b) The differences compared to (a) are that higher concentrations of trypsin (10 μM) and Ac-TVASSSTA-complexed PAI-1 (3 μM) were used and that the reaction was monitored over a shorter period of time. The reaction components were separated by SDS−PAGE into (1) the acyl enzyme intermediate, (2) unreacted, free, and noncovalently bound PAI-1, and (3) PAI-1 hydrolyzed at the scissile bond. The contents of the corresponding bands were quantitated and plotted against time. The solid lines represent single exponentials with the best fit exponential rate constant k_{obs} = 23 ± 3 s^{-1} for the decay of unreacted PAI-1 (■), free or noncovalently bound, and k_{obs} = 21 ± 2 s^{-1} for the growth of PAI-1 hydrolyzed at the scissile bond (▲). The acyl enzyme intermediate has been indicated (●).

bifurcation scheme. The hydrolyzed form does not, however, derive from a preexisting substrate form of PAI-1. The evidence collected in support of this statement is both qualitative and quantitative. With enzyme in excess over inhibitor, different amounts of hydrolyzed PAI-1 were observed depending on whether tPA or trypsin was used (cf. gels in Figures 2 and 5). The amount of hydrolyzed PAI-1 observed by SDS−PAGE after reacting the inhibitor with trypsin was dependent on the pH of the reaction medium but independent of whether PAI-1 or trypsin was used in excess (Figure 1). Moreover, the ratio of hydrolyzed to complexed PAI-1 was independent of the reaction time with both tPA and trypsin.

The Apparent Second-Order and Limiting Rate Constants for Acylation of Trypsin by Inhibitor and Substrate PAI-1. The apparent second-order rate constant for binding PAI-1 to trypsin, k_{app}, was determined to be 2.80 ± 0.01 s^{-1} μM^{-1} as described above. The rapid acid quenching technique and SDS−PAGE were applied to determine the limiting rate constant for acylation of trypsin by PAI-1. With 10 μM trypsin and 1 μM PAI-1, the rate constant for formation of the stable complex was 19 s^{-1} (Figure 2). The decrease of free PAI-1 and the increase of minor amounts of scissile bond hydrolyzed PAI-1 followed the same time course. Increasing the concentration of trypsin to 20 μM had only a small effect on the rate constant, which increased to 21 s^{-1}, a value which was taken to represent k_{lim} for acylation of trypsin by inhibitor PAI-1.

The second-order rate constant for productive binding of substrate PAI-1 to trypsin was determined by the rapid acid quenching technique, using subsaturating amounts of substrate PAI-1 and catalytic amounts of trypsin. As expected, this resulted in an exponential decay of substrate PAI-1 into the scissile bond hydrolyzed product (Figure 3). The rate constant reported in the figure legend, which equals V_{max}/K_m, gave an apparent second-order rate constant for productive binding of substrate PAI-1 to trypsin, $k_{app} = k_{cat}/K_m$ = 2.9 ± 0.1 μM^{-1} s^{-1}, on the basis of the enzyme concentration used. This indicates that blocking loop insertion in PAI-1 has no effect on its overall reactivity with trypsin.

To measure the limiting rate constant for acylation of trypsin by substrate PAI-1, single turnover measurements were performed with trypsin in excess over substrate PAI-1. Under such conditions, scissile bond hydrolyzed PAI-1 should increase by a single exponential with a rate constant that approaches k_{cat} at increasing concentrations of the enzyme. Using 5 μM trypsin and 1.6 μM substrate PAI-1, the rate constant observed for the formation of reactive center bond hydrolyzed PAI-1 (Figure 4A) was ~13 s^{-1}. To attempt to saturate this rate constant and demonstrate that

the faint, transient band observed at the migration position for the stable complex formed with trypsin and inhibitor PAI-1 is the acyl enzyme intermediate, the experiment was repeated using 3 μM substrate PAI-1 and 10 μM trypsin and data was collected over a shorter time. As indicated by the data in Figure 4b, this approach made transient accumulation of the acyl enzyme intermediate more obvious. Throughout the reaction only a fraction of total PAI-1 was confined to the acyl enzyme intermediate, indicating that acylation limits turnover of trypsin with substrate PAI-1. On the basis of the individual quantitation of the bands carrying hydrolyzed and intact PAI-1, respectively, only a moderate increase to 21−23 s^{-1} in the overall reaction rate was observed, indicating that with a 10 μM concentration of the excess reactant the system is nearly saturated and that k_{lim} for the acylation of trypsin by substrate PAI-1 attains a value close to the 21 s^{-1} reported above for the acylation of trypsin by inhibitor PAI-1. To investigate the effect of the excess trypsin on the stable acyl enzyme formed with inhibitor PAI-1, trypsin (10 μM) was incubated with inhibitor PAI-1 (1 μM) and subjected to acid quenching after prolonged lengths of time. A single-step degradation of the complex was observed that resulted in a species running only slightly lower on the gel than the complex first established and was completed after only several minutes of incubation.

The Apparent Second-Order and Limiting Rate Constants for Acylation of tPA by Inhibitor and Substrate PAI-1. The apparent second-order rate constant, k_{app}, for the overall reaction of inhibitor PAI-1 with tPA was determined to be 13 μM^{-1} s^{-1} as described in the Experimental Section. In a subsequent experiment, the PAI-1 concentration was increased 100-fold to 4 μM and the reaction with 2 μM tPA was monitored by the rapid quenching technique in combination with SDS−PAGE (Figure 5). Despite the fact that the concentrations chosen do not sustain a pseudo-first-order reaction, the stable acyl enzyme intermediate increased by a single exponential, suggesting that the reaction was saturated. This was corroborated by the associated rate constant, which was only 3.3 ± 0.8 s^{-1} and consequently was taken as k_{lim} for the reaction of inhibitor PAI-1 with tPA. We have previously reported that a rate constant of 3.4 s^{-1} limits the fluorescence change associated with the reaction of tPA with the P9 Ser→Cys mutant PAI-1, carrying a fluorescent label at the mercapto group, and which was shown to be associated with insertion of the RCL into β-sheet A (*9*). The almost identical limiting values for acylation and cleaved RCL insertion provide evidence that the two processes are limited by the same step. To investigate whether this step depends directly on base catalysis by His-57, a rapid quenching study was performed at pH 6.15. At this pH, k_{app} for binding inhibitor PAI-1 to tPA was found to be reduced to 1.6 μM^{-1} s^{-1}. Despite this, acylation of 1.5 μM tPA by 3 μM PAI-1 was complete in less than 1 s, indicating a significant increase in k_{lim} at pH 6.15 compared to that at pH 7.5 (cf. time scale in Figure 5). No attempts were made to saturate the reaction or establish pseudo-first-order conditions. Further measurements were performed at pH 7.5 using a commercial preparation of tPA (Activase), which contains sc- and tc-tPA in a proportion of about 8:2. Unlike the single-chain precursor of most mammalian serine proteinases, single-chain tPA is an active enzyme. Plasmin activation of tPA to its two-chain form, however, has been

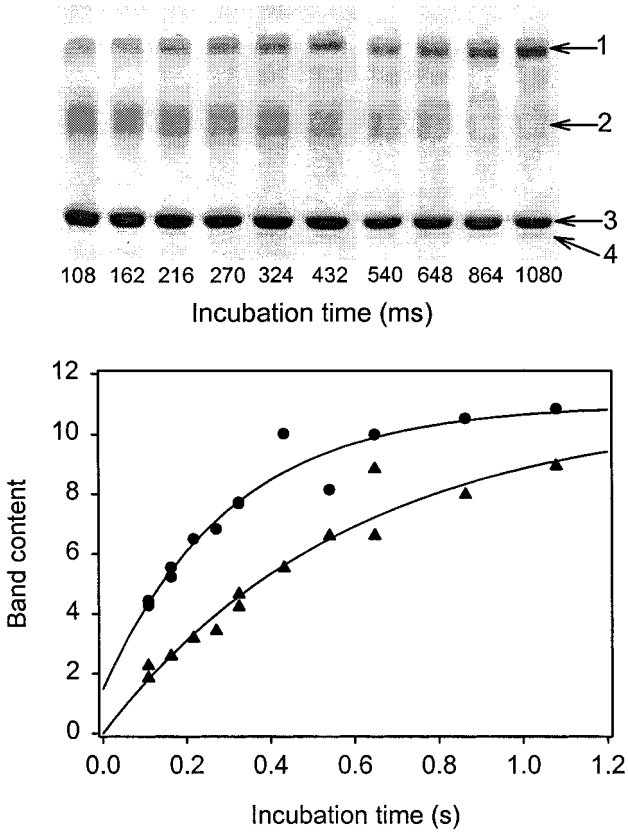

FIGURE 5: Time course for acylation of tPA by inhibitor PAI-1 under saturating conditions. Data were obtained by the rapid quenching technique in combination with SDS−PAGE. The gel demonstrates the progressive formation of the stable tPA·PAI-1 acyl enzyme complex in the reaction of 4 μM inhibitor PAI-1 with 2 μM plasmin-activated, two-chain tPA. The bands on the gel are (1) the tPA·PAI-1 complex, (2) tPA, (3) unreacted PAI-1, free and noncovalently bound, and (4) PAI-1 hydrolyzed at the scissile bond. (The diffuse nature of the tPA band is caused by a heterogeneity in sialic acid content). The tPA·PAI-1 bands were quantitated and plotted against time (●). The associated solid line is a single exponential with the best fit rate constant k_{obs} = 3.3 ± 0.8 s^{-1}. Data obtained under identical conditions except for the use of a commercial preparation of tPA (Activase), which contains mainly single-chain tPA, has been included (▲). The associated rate constant was determined as k_{obs} = 1.7 ± 0.6 s^{-1}.

shown to increase its k_{cat} for the hydrolysis of chromogenic substrates, a reaction limited by enzyme acylation, by a factor of 2−3 (*37*). Rapid quenching measurements at pH 7.5 of PAI-1 binding to Activase instead of to two-chain tPA gave a limiting rate constant for acylation which was reduced 2-fold to 1.7 ± 0.3 s^{-1} (Figure 5).

The apparent second-order rate constant for the overall reaction of substrate PAI-1 with tPA was determined spectrophotometrically using the competitive hydrolysis of Spectrozyme^{tPA} as a reporter reaction (Figure 6). This approach was both necessary and feasible because of much lower k_{cat} and K_m values than those for the corresponding reaction with trypsin. Complete hydrolysis of substrate PAI-1 (0.1 and 0.2 μM) was observed as a lag in hydrolysis of the chromogenic substrate. The data was evaluated as described in the Experimental Section and gave k_{cat} = 0.059 s^{-1} and K_m = 0.024 μM for the hydrolysis of the scissile bond in PAI-1 by two-chain tPA. Using these numbers, the calculated k_{app} for binding substrate PAI-1 to tPA is 2.5 μM^{-1} s^{-1}. The 5-fold reduction of k_{app} compared to that measured

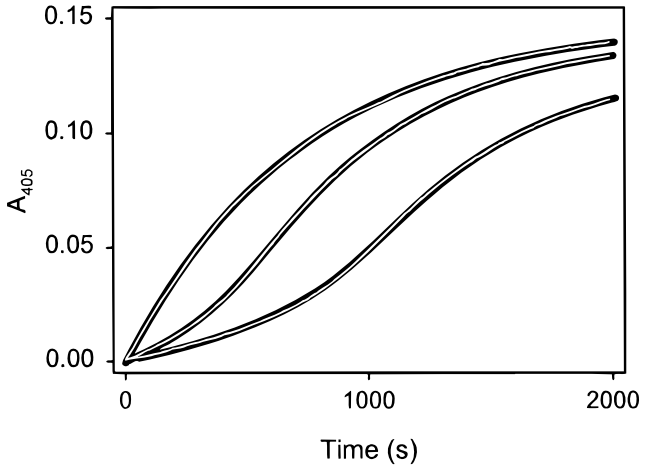

FIGURE 6: Indirect photometric recordings of the complete hydrolysis of substrate PAI-1 by tPA, using a competitive chromogenic substrate. The enzyme (0.005 μM) was reacted with 0 (top curve), 0.1 (center curve), and 0.2 (bottom curve) μM PAI-1 complexed with Ac-TVASSSTA in the presence of 14 μM Spectrozyme^{tPA}, the hydrolysis of which was monitored at 405 nm (superimposed white curves). The kinetic parameters for hydrolysis of substrate PAI-1 were evaluated by fitting the implicit function in eq 1 to the absorbance progress curves. With 0.1 μM substrate PAI-1, V_b was evaluated to be 3.11×10^{-4} μM s^{-1} and with 0.2 μM, it was slightly lower at 2.74×10^{-4} μM s^{-1}, whereas K_b was evaluated at 0.024 μM in both instances. The black lines represent eq 1 using best fit parameter values.

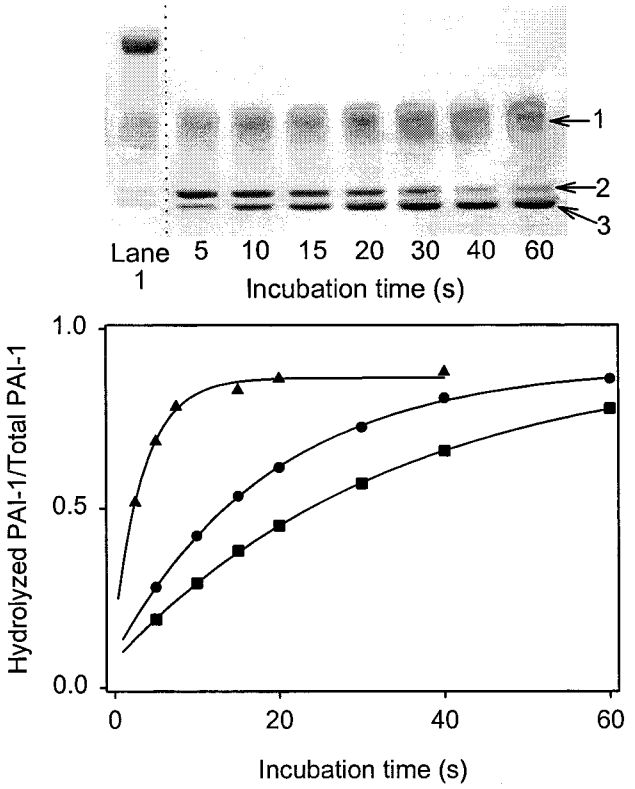

FIGURE 7: Saturated time courses for hydrolysis of substrate PAI-1 by tPA under single turnover conditions. Data were obtained by the rapid acid quenching technique in combination with SDS−PAGE. The gel demonstrates the progressive hydrolysis of 2 μM PAI-1 complexed with Ac-TVASSSTA by 3 μM plasmin-activated, two-chain tPA under standard conditions at pH 7.5 (lane 1 has been included to indicate the position of the stable complex of tPA and inhibitor PAI-1). The quantitative evaluation of the gel reported formation of hydrolyzed PAI-1 (●) by a single exponential with the best fit rate constant $k_{obs} = 0.053 \pm 0.002$ s^{-1}. The lower curve (■) was obtained under the same conditions, but with Activase instead of plasmin-activated two-chain tPA. The corresponding rate constant was $k_{obs} = 0.029 \pm 0.001$ s^{-1}. The upper curve (▲) was obtained using the plasmin-activated, two-chain tPA, but with the reaction performed at a pH reduced to 6.15. The best fit rate constant at pH 6.15 was $k_{obs} = 0.27 \pm 0.04$ s^{-1}.

with inhibitor PAI-1 indicates that the overall reactivity of tPA with PAI-1, in contrast to that of trypsin, depends on loop insertion.

If acylation is rate limiting, the k_{cat} determined with tPA would indicate that the physiological target enzyme is acylated at least 50 times more slowly by substrate PAI-1 than by unmodified PAI-1. To obtain direct information about the relative rates of acylation and deacylation in the reaction of tPA with substrate PAI-1, the Ac-TVASSSTA-complexed substrate PAI-1 (2 μM) was reacted with tPA (3 μM) and the reaction was quenched at increments of 5 s (Figure 7). Under such conditions and on the basis of k_{cat} and K_m, saturation of the Michaelis complex should occur within less than 1 s, leaving a minimum of 1 μM tPA free. This concentration is 20 times the K_m, which means that the reaction monitored was the decomposition of a saturated Michaelis complex into the hydrolyzed inhibitor and free enzyme. The gel in Figure 7, separating the reaction components formed at the consecutive 5-s intervals, shows that the decay of the Michaelis complex (dissociated into free tPA and PAI-1 by SDS−PAGE) occurred in a single-exponential phase without accumulation of detectable amounts of the acyl enzyme intermediate, indicating that the reaction is not limited by deacylation. The rate constant determined for the process was 0.053 s^{-1}, very close to the k_{cat} determined with the competitive chromogenic substrate technique (0.059 s^{-1}) and thereby confirming that the Michaelis complex was saturated. At pH 6.15, k_{lim} increased 5-fold to 0.27 s^{-1} (Figure 7), which is consistent with the corresponding data reported above for inhibitor PAI-1. Just as with inhibitor PAI-1, k_{lim} decreased by a factor of 2 when Activase was used instead of tPA (Figure 7).

The kinetic parameters determined for the reactions of inhibitor and substrate PAI-1 with tPA and trypsin are summarized in Table 1.

Table 1: Kinetic Parameters[a] Determined for the Reactions of PAI-1 and Substrate PAI-1 with tPA and Trypsin

target enzyme	k_{app} (μM^{-1} s^{-1})	k_{lim} (s^{-1})	K_m (μM)
tPA	13 (2.5)[c]	3.3 (0.059)	0.25[b] (0.024)
trypsin	2.8 (2.9)	21 (21)	7.5[b] (7.2)

[a] Based on measurements at pH 7.5, 25 °C and 0.15 M ionic strength. [b] Calculated as k_{lim}/k_{app}. [c] Values within parentheses were obtained with substrate PAI-1.

To investigate the possibility that loop−sheet interactions prior to covalent bond formation contribute to the higher rate of acylation of tPA by inhibitor PAI-1 than by the loop constrained substrate form, a stopped-flow experiment was designed to compare the kinetics of the noncovalent binding of the two PAI-1 forms to tPA. The experiment consisted of reacting the respective PAI-1 form (1 μM) with excess tPA (1.8 μM) in the presence of Spectrozyme^{tPA} (80 μM). On the basis of the acylation rates presented above, the half-life of the Michaelis complex with respect to covalent bond formation exceeds 200 ms with inhibitor PAI-1 and is much longer with peptide-blocked PAI-1. The data presented in Figure 8 show that the effect of the two PAI-1 forms on the

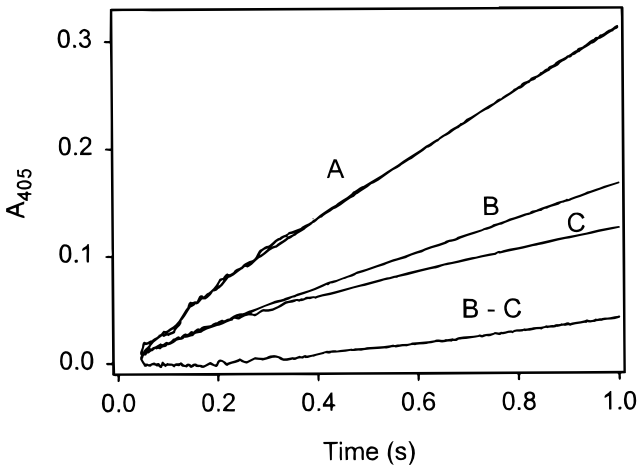

FIGURE 8: Inhibition of tPA by noncovalent binding of inhibitor and substrate PAI-1. Stopped-flow photometric recordings of the reactions of tPA (1.8 μM) with Spectrozyme^{tPA} (80 μM) in the absence (A) and presence (B) of substrate PAI-1 (1 μM) or (C) inhibitor PAI-1 (1 μM). Note the coincidence of curve B and C over the first 200 ms of the reaction, an interval in which enzyme acylation is insignificant, and the progressive divergence of the two curves in the course of enzyme acylation, leading to hydrolysis of substrate PAI-1 with concomitant liberation of tPA and to a stable complex with inhibitor PAI-1.

chromogenic reaction was virtually identical for the first 200 ms, rapidly reducing its rate by ~50%. This indicates that over a period of time in which covalent bond formation is only a minor factor, binding of the two PAI-1 forms to tPA is virtually identical. After this initial phase, tPA was progressively less inhibited by substrate PAI-1 than by inhibitory PAI-1, which is consistent with the slow breakdown of the Michaelis complex formed with substrate PAI-1 ($t_{1/2}$ = 12 s) and the additional stabilization of the complex formed with inhibitor PAI-1 through covalent bond formation.

DISCUSSION

The trapping of the acyl enzyme intermediate at low pH in the reaction of trypsin with the peptide-blocked substrate PAI-1 is a direct demonstration of the classical mechanism for serine proteinase catalysis, illustrated by the substrate branch in Scheme 1. The transient nature of the acyl enzyme intermediate emphasizes that, without the capability of loop insertion, PAI-1 exposes a reactive center bond which is highly susceptible to hydrolysis by trypsin, an enzyme which is completely inhibited by unmodified PAI-1 and which is the prototype for the PAI-1 physiological target enzymes, the tissue- and urinary-type plasminogen activators. The second-order and limiting rate constants (k_{app} and k_{lim}) governing formation of the stable complex of trypsin and inhibitor PAI-1 were indistinguishable from those governing formation of the acyl enzyme intermediate with trypsin and substrate PAI-1. This shows that when trypsin is the target, k_1, k_{-1}, and k_2 are indifferent to blocking position 4 in β-sheet A of the serpin, in accordance with the mechanism in Scheme 1. It further indicates that the reactive center is equally exposed in inhibitor and peptide-blocked PAI-1 and that the RCL is fully extracted from β-sheet A in free PAI-1 and its Michaelis complex with trypsin.

The corresponding data obtained with tPA, however, were different. Although the two PAI-1 forms exhibited the same

Scheme 3

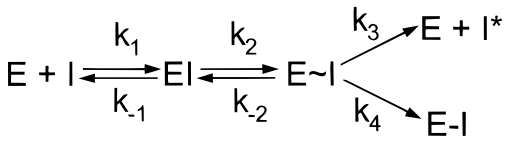

reactivity toward tPA with regard to forming the Michaelis complex, which corroborates that inhibitor PAI-1 is characterized by a fully extracted RCL, tPA was acylated 57 times more slowly by substrate PAI-1 than by inhibitor PAI-1. This is not consistent with the mechanism in Scheme 1, in which loop insertion is triggered by an irreversible step of enzyme acylation. If this mechanism were operative, loop insertion could have no effect on the acylation rate constant, which would be equal to k_2 with both inhibitor and substrate PAI-1. The apparently controversial results obtained with trypsin and tPA can be resolved by assuming that bifurcation of the reaction is preceded by a readily reversible step of enzyme acylation as indicated in Scheme 3. Following saturation of the Michaelis complex, relaxation of the reaction system in Scheme 3 will be governed by two exponential transients. On the basis of a mathematical description presented in ref 38, the corresponding rate constants are the roots, r_1 and r_2, of the quadratic equation $r^2 - r(k_2 + k_{-2} + k_{ir}) + k_2k_{ir} = 0$, where k_{ir} is the rate constant for the irreversible step(s) and equals k_3 with the substrate serpin and $k_3 + k_4$ with the unmodified inhibitor. In most instances $r_1 \gg r_2$, such that $r_1 \cong k_2 + k_{-2} + k_{ir}$ and $r_2 \cong k_2k_{ir}/r_1$. An exception occurs if $k_{ir} \gg k_{-2}$. This situation, however, would make the mechanism in Scheme 3 indistinguishable from that in Scheme 1 and, hence, can explain the results obtained with trypsin but not those obtained with tPA.

In the reactions of tPA with PAI-1, the acyl enzyme intermediate was not observed, either as a transient intermediate (with substrate PAI-1) or as a burst phase of stable complex formation (with inhibitor PAI-1). This means that formation of the acyl enzyme is much slower than its breakdown or stabilization, or, in terms of rate constants, that $k_{-2} + k_{ir} \gg k_2$. It follows that the limiting rate constant determined for acylation of tPA by inhibitor and substrate PAI-1 corresponds to r_2, the slower of the two transients, now reduced to the expression in eq 2. Because blocking

$$k_{lim} = r_2 \cong k_2k_{ir}/(k_{-2} + k_{ir}) \quad (2)$$

β-sheet A in PAI-1 did not affect the Michaelis complex formed with tPA, the intrinsic forward reactivity of this complex, symbolized by k_2 in Scheme 3, should be the same with inhibitor and substrate PAI-1, as it was when trypsin was the target. On the basis of the limiting rate constant determined for acylation of tPA by inhibitor PAI-1, k_2 is 3.3 s^{-1} or larger (cf. eq 2). With substrate PAI-1, k_{ir} equals k_3, which means that eq 2 can be solved for the ratio of k_{-2} to k_3. Using 3.3 s^{-1} for k_2 and 0.059 s^{-1} for k_{lim}, the result is k_{-2}/k_3 ($= k_2/k_{lim} - 1$) = 56, which clearly indicates that $k_{-2} \gg k_3$. Hence, in the reaction of tPA with substrate PAI-1, the Michaelis complex and the acyl enzyme can be considered to establish an equilibrium which greatly favors the Michaelis complex. Further limitations are imposed by the observation (Figures 2 and 5) that the proportion of

inhibitor PAI-1 that was hydrolyzed in the reactions with tPA was much less than unity. Because this proportion is given by $k_3/(k_3 + k_4)$, we have $k_4 \gg k_3$. With these constraints, the relative effect of loop insertion on the limiting rate constant for enzyme acylation by PAI-1 can be calculated using eq 3. In eq 3, k_{inh} and k_{cat} are used to distinguish the

$$\frac{k_{inh}}{k_{cat}} = \frac{k_2(k_3 + k_4)}{k_{-2} + (k_3 + k_4)} \Bigg/ \frac{k_2 k_3}{k_{-2} + k_3} \overset{(k_{-2},k_4 \gg k_3)}{\cong} \frac{k_4}{k_3}\left(\frac{k_{-2}}{k_{-2} + k_4}\right) \tag{3}$$

limiting rate constants for acylation of tPA by inhibitor and substrate PAI-1, respectively. Eq 3 demonstrates that loop insertion in PAI-1 will increase the limiting rate constant for acylation of tPA by a factor which ranges from k_{-2}/k_3 to k_4/k_3 depending on the relative magnitude of k_{-2} and k_4. If $k_{-2} \gg k_4$, then the Michaelis complex and the acyl enzyme formed with inhibitor PAI-1 approach the same unfavorable equilibrium they establish when formed with substrate PAI-1. This is the kinetic situation in which the system makes optimal use of loop insertion to accelerate enzyme acylation.

The expression for the apparent second-order rate constant for PAI-1 binding according to the mechanism in Scheme 3 presented in eq 4a was derived with the assumption that the

$$k_{app} = \frac{k_1 k_2 k_{ir}}{k_{-1}k_{-2} + k_{-1}k_{ir} + k_2 k_{ir}} \tag{4a}$$

change with time of the intermediates is negligible compared to the depletion in reactants and growth of products. Potential effects of loop insertion on k_{app} are more clearly demonstrated by substituting the reduced expression for k_{lim} in eq 2 into eq 4a:

$$k_{app} = \frac{k_1 k_{lim}}{k_{-1} + k_{lim}} \tag{4b}$$

As mentioned above, the results with trypsin are consistent with Scheme 3 assuming that $k_{ir} \gg k_{-2}$ with this enzyme. The corresponding expression for k_{app} is obtained by replacing k_{lim} in eq 4b with k_2. Hence, the mechanism in Scheme 3, but not that in Scheme 1, can explain the difference observed in the second-order rate constants for acylation of tPA by inhibitor and substrate PAI-1, 13 vs 2.5 μM^{-1} s^{-1}, as well as the absence of such a difference in the corresponding rate constants for the reactions of the two PAI-1 forms with trypsin. Scheme 3 also explains why the difference in k_{app} is reduced relative to the difference in k_{lim}. Using the values reported in Table 1 for the reaction with tPA, that is, 3.3 and 0.053 s^{-1} for k_{lim} and 13 and 2.5 μM^{-1} s^{-1} for k_{app} with inhibitor and substrate PAI-1, respectively, we have the identity in eq 5. Evaluation of eq 5 sets the

$$2.5\left(\frac{k_1 3.3}{k_{-1} + 3.3}\right) = 13\left(\frac{k_1 0.059}{k_{-1} + 0.059}\right) \tag{5}$$

rate constant for dissociation of the Michaelis complex formed with tPA to $k_{-1} = 0.27$ s^{-1}. Substituting k_{-1} in eq 4b for 0.27 gives $k_1 = 14$ μM^{-1} s^{-1}. Thus, the K_d for the noncovalent binding of PAI-1 to tPA is 19 nM, consistent with the K_m of 24 nM for hydrolysis of substrate PAI-1 by tPA, reported in Table 1, and in reasonable agreement with the K_d of 50 nM previously estimated for the binding of PAI-1 to diisopropyl phosphofluoridate-inhibited tPA (*16*) and the K_d of 5 nM reported for the interaction of PAI-1 with the inactive Ser-195→Ala mutant tPA (*39*).

The physical basis for why tPA, but not trypsin, is acylated faster by inhibitor PAI-1 than by the substrate form must be traced to residues in tPA which are different or absent in trypsin and which can have a strong influence on the interaction of the proteinase with PAI-1. Several serpin systems, including that of PAI-1 and tPA, depend on exosite interactions, either direct or via a template like heparin, for fast binding to the physiological target proteinase (*16*, *20*, *40*). A corollary of the serpin reaction mechanism is, however, that all bonds between enzyme and inhibitor established in the Michaelis complex must be broken or distorted before strand 4, carrying the proteinase, can insert into β-sheet A and complete the inhibitory reaction path (*10*, *11*). As a consequence, to the extent that such exosite interactions prevent dissociation of the proteinase·serpin Michaelis complex, they should also make it less prone to react in the forward direction, if this involves breaking the exosite bonds.

The salt bridge between Glu-350 (P4′) in PAI-1 and Arg-39 in tPA (*20*, *21*) directly affects binding of the distal part of the RCL to the active site cleft in tPA. This part of the RCL is firmly integrated with the main body of the inhibitor (*5*, *6*), a fact which makes bonds between this fragment and the enzyme substrate pocket significant for several reasons. They must be broken before the reaction can proceed toward scissile bond hydrolysis or acyl enzyme stabilization, and stronger or weaker, they should have no effect on PAI-1 inhibitory efficiency. They will stabilize the Michaelis complex toward both dissociation and acylation, the latter by retaining the α-amino group on P1′ in the substrate pocket, and facilitate the reverse deacylation. The proximal part of the RCL, on the other hand, becomes covalently attached to the proteinase in the acylation step, and additional bonds between the enzyme and this part of the RCL will not stabilize the Michaelis complex toward acylation. Strong interactions between the substrate pocket of the target enzyme and the distal part of the RCL are likely to play a vital role for the preservation of the scissile bond in the reaction of the canonical inhibitor and should have a similar influence in the reaction of PAI-1 with tPA. However, the much longer and more flexible proximal portion of the serpin RCL compared to that of the canonical inhibitor will shift the equilibrium toward acylation by facilitating a separation of the products of the acylation step. Our results indicate that loop insertion provides an effective means for driving this separation, reducing the half-life of the Michaelis complex from 12 to 0.21 s. The substrate form of PAI-1 lacks such means and should therefore have properties closer to those of the canonical inhibitor, with tight binding and slow turnover, a prediction confirmed by this study.

Deacylation by the P1′ α-amino group is an unlikely event once it has been separated from the enzyme substrate pocket because of the high concentration of the competing water, protonation of the α-amino group, and removal of the enzyme through loop insertion. Nevertheless, our results show that bifurcation of the PAI-1 reaction with tPA is triggered by a reversible step of enzyme acylation. We must therefore assume that bifurcation is triggered in the acyl

enzyme intermediate, in which the distal fragment of the RCL is still bound to the active site cleft. Therefore, k_3 and k_4 in Scheme 2 become compound rate constants that, apart from aqueous deacylation and loop insertion, respectively, account for the separation of the distal RCL fragment from the enzyme by two different mechanisms, its passive displacement by bulk water (k_3) and the active separation achieved by the pulling action of the inserting loop on the enzyme (k_4). Support for this mechanism was provided by measurements performed at pH 6.15 instead of at pH 7.5 or which used the predominantly single-chain tPA contained in Activase instead of two-chain tPA. When the pH was reduced from 7.5 to 6.15, k_{inh} and k_{cat}, the limiting rate constants for acylation of tPA by inhibitor and substrate PAI-1, respectively, both increased. This indicates that k_{inh} and k_{cat} are not limited by the covalent bond breaking steps in acylation or deacylation, because these depend on a neutral His-57 and hence should be reduced at pH 6.15 compared to pH 7.5. The observation that the proportion of hydrolyzed PAI-1 generated in the reaction with tPA did not increase at pH 6.15 compared to pH 7.5 provides additional support that k_3 and k_4 are limited by the same step. When Activase was used as target, k_{inh} and k_{cat} were both reduced by a factor of 2. According to eq 2, k_{inh} and k_{cat} are directly proportional to k_2. Hence, a higher k_2 in the reactions of PAI-1 with two-chain tPA than in those with the single-chain form can explain the different limiting rates seen with Activase.[5] It would be consistent with the higher k_{cat} reported for chromogenic substrate hydrolysis by two-chain tPA than that for hydrolysis by the single-chain form (*37*).

The primary effect of the exosite interactions associated with complementary charged amino acid residue side chains in tPA and PAI-1 should be to increase k_1, an assumption consistent with the demonstration that mutant forms of tPA which lack one or several of the positively charged residues in the 37-loop exhibit reduced rates of inhibition by PAI-1 (*17*). If the exosite bonds remain intact in the Michaelis complex—and this should apply at least to the bond between the P4′ Glu and Arg39 in tPA—they will hamper the reactivity of the Michaelis complex in all directions that depend on breaking the exosite bonds, such as forming a stabilized acyl enzyme complex through loop insertion and a concomitant translocation of the proteinase. This reduction of the forward reaction rate, however, is more than offset by a mechanism which uses the large free energy associated with loop insertion to decrease the potential of the acyl enzyme intermediate relative to that of the Michaelis complex (strand 4 must be completely extracted from β-sheet A in order to reestablish the scissile bond in a monomolecular reaction step). Assuming that the relative magnitudes of rate constants are not drastically altered at 37 °C, it appears that k_{lim} has been maximized, because it already exceeds k_{-1} and a further increase would according to eq 4b have no impact on k_{app}, the "specificity" rate constant for PAI-1 binding. With trypsin as target, on the other hand, the kinetic barrier separating the Michaelis complex from the acyl enzyme appears to be low such that loop insertion is of little help in crossing this barrier, consistent with the absence of strong exosite interactions as well as with the broader specificity and higher reactivity of trypsin.

In conclusion, this study has demonstrated that insertion of the tPA-cleaved RCL of PAI-1 into β-sheet A of the inhibitor, resulting in inhibition of the enzyme, is triggered by a freely reversible step of enzyme acylation. Evidence has been presented indicating that tight binding of the distal part of the cleaved RCL of PAI-1 to tPA accounts for an intrinsically unfavorable acylation step and limits the rate of the overall reaction. Our data has provided evidence that the RCL of PAI-1 is fully extracted from β-sheet A in the free serpin as well as in its Michaelis complex with both tPA and trypsin.

[5] The results at pH 6.15 and with Activase are consistent with $k_4 \ll k_{-2}$, a possibility discussed in connection with eq 3. Because k_{-2}, $k_4 \gg k_3$, eq 2 reduces to $k_{inh} = k_4k_2/k_{-2}$ and $k_{cat} = k_3k_2/k_{-2}$, when expressed for inhibitor and substrate PAI-1, respectively. The indentical relative reduction in k_{inh} and k_{cat} observed with Activase would be due to a less favorable k_2/k_{-2} ratio with the single-chain tPA. The faster acylation of tPA by both inhibitor and substrate PAI-1 at pH 6.15 could be due to a pH effect on the dissociative step common to k_3 and k_4, or to a lower pK_a of His-57 in the Michaelis complex than in the acyl enzyme, which would increase the k_2/k_{-2} ratio at pH 6.15 relative to that at pH 7.5.

SUPPORTING INFORMATION AVAILABLE

Detailed description of the rapid quenching apparatus and its application in the continuous- and pulsed-flow modes (1 page). Ordering information given on any current masthead page.

REFERENCES

1. Carrell, R. W., and Travis, J. (1985) *Trends. Biochem. Sci. 10*, 20−24.
2. Wei, A., Rubin, H., Cooperman, B. S., and Christianson, D. W. (1994) *Nat. Struct. Biol. 1*, 251−258.
3. Björk, I., Nordling, K., and Larsson, I. (1992) *J. Biol. Chem. 267*, 19047−19050.
4. Kvassman, J.-O., Lawrence, D. A., and Shore, J. D. (1995) *J. Biol. Chem. 270*, 27942−27947.
5. Loebermann, H., Tokuoka, R., Deisenhofer, J., and Huber, R. (1984) *J. Mol. Biol. 177*, 531−556.
6. Mottonen, J., Strand, A., Symersky, J., Sweet, R., Danley, D. E., Geoghegan, K., Gerard, R. D., and Goldsmith, E. J. (1992) *Nature 355*, 270−273.
7. Nilson, T., and Wiman, B. (1982) *FEBS Lett. 142*, 111−114.
8. Lawrence, D. A., Ginsburg, D., Day, D. E., Berkenpas, M. B., Verhamme, I., Kvassman, J.-O., and Shore, J. D. (1995) *J. Biol. Chem. 270*, 25309−25312.
9. Shore, J. D., Day, D. E., Francis-Chmura, A. M., Verhamme, I., Kvassman, J.-O., Lawrence, D. A., and Ginsburg, D. (1995) *J. Biol. Chem. 270*, 5395−5398.
10. Wright, H. T., and Scarsdale, J. N. (1995) *Proteins: Struct., Funct. Genet. 22*, 210−225.
11. Wilczynska, M., Fa, M., Karolin, J., Ohlsson, P.-I., Johansson, L. B.-Å., and Ny, T. (1997) *Nat. Struct. Biol. 4*, 354−357.
12. Walsh, C., Cromartie, T., Marcotte, P., and Spencer, R. (1978) *Methods Enzymol. 53*, 437−448.
13. Hartley, B. S., and Kilby, B. A. (1954) *Biochem. J. 56*, 288−297.
14. Rubin, H., Wang, Z. M., Nickbarg, E. B., McLarney, S., Naidoo, N., Schoenberger, O. L., Johnsson, J. L., and Cooperman, B. S. (1990) *J. Biol.Chem. 265*, 1199−12−7.
15. Chaillan-Huntington, C. E., Gettins, P. G. W., Huntington, J. A., and Patson, P. A. (1997) *Biochemistry 36*, 9562−9570.
16. Chmielewska, J., Rånby, M., and Wiman, B. (1988) *Biochem. J. 251*, 327−332.
17. Tachias, K., and Madison, E. L. (1997) *J. Biol. Chem. 272*, 14580−14585.
18. Lamba, D., Bauer, M., Huber, R., Fisher, S., Rudolph, R., Kohnert, U., and Bode, W. (1996) *J. Mol. Biol. 258*, 117−153.
19. Horrevoets, A. J., Tans, G., Smilde, A. E., van Zonneveld, A. J., and Pannekoek, H. (1993) *J. Biol. Chem. 268*, 779−782.

20. Madison, E. L., Goldsmith, E. J., Gerard, R. D., Gething, M.-J. H., and Sambrook, J. F. (1989) *Nature 339*, 721−724.
21. van Meijer, M., Roelofs, Y., Neels, J., Horrevoets, A. J. G., van Zonneveld, A.-J., and Pannekoek, H. (1996) *J. Biol. Chem. 271*, 7423−7428.
22. Barman, T. E., and Gutfreund, H. (1965) *Proc. Natl. Acad. Sci. U.S.A. 53*, 1243−1245.
23. Kvassman, J.-O., Verhamme, I., and Shore, J. D. (1997) in *Chemistry and Biology of Serpin*s (Church, F. C., Cunningham, D. D., Ginsburg, D., Hoffman, M., Stone, S. R., and Tollefsen, D. M., Eds.) p 293, Plenum Press, New York.
24. van Boeckel, C. A. A., Grootenhuis, P. D. J., and Visser, A. A. (1994) *Nat. Struct. Biol. 1*, 423−425.
25. Carrell, R. W., Stein, P. E., Fermi, G., and Wardell, M. R. (1994) *Structure 2*, 257−270.
26. Huntington, J. A., Olson, S. T., Fan, B., and Gettins, P. G. W. (1996) *Biochemistry 35*, 8495−8503.
27. Wallén, P., Bergsdorf, N., and Rånby, M. (1982) *Biochim. Biophys. Acta 719*, 318−328.
28. Vaughan, D. E., Declerk, P. J., Reilly, T. M., Park, K., Collen D., and Fasman, G. D. (1993) *Biochim. Biophys. Acta 1202*, 221−229.
29. Tian, W. X., and Tsou, C. L. (1982) *Biochemistry 21*, 1028−1032.
30. Willstätter, R., Kuhn, R., Lind, O., and Memmen, F. (1927) *Z. Physiol. Chem. 167*, 303.
31. Dixon, M., and Webb, E. C. (1964) in *Enzymes*, 2nd ed., pp 84−87, Academic Press, New York.
32. Blake, R. C., II, Vassall, R. F., and Blake, D. A. (1989) *Arch. Biochem. Biophys. 272*, 52−68.
33. Blow, D. M. (1971) *The Enzymes*, 3rd ed., pp 185−212.
34. Hess, G. P. (1971) *The Enzymes*, 3rd ed., pp 213−248.
35. Fersht, A. R., and Requena, Y. (1971) *J. Am. Chem. Soc. 93*, 7079−7087.
36. Marquart, M., Walter, M. J, Deisenhofer, J., Bode, W., and Huber, R. (1983) *Acta Crystallogr. B39*, 480.
37. Fisher, B. E. (1992) *Blood Cogulation Fibrinolysis 3*, 197−204.
38. Capellos, C., and Bielski, B. H. J. (1972) in *Kinetic Systems Mathematical Description of Chemical Kinetics in Solution*, pp 35−38, Wiley-Interscience, John Wiley and Sons Inc., New York.
39. Lijnen, R. H., Van Hoef, B., and Collen, D. (1991) *J. Biol. Chem. 266*, 4041−4044.
40. Björk, I., and Nordenman, B. (1976) *Eur. J. Biochem. 68*, 507−511.

BI9814787